Heliyon 10 (2024) e36816

Contents lists available at ScienceDirect

Heliyon

journal homepage: www.cell.com/heliyon

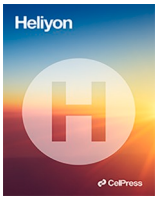

Research article

Identification of costimulatory molecule signatures for evaluating prognostic risk in non-small cell lung cancer

Yan Yang, Suqiong Lu, Guomin Gu *

Department of Pulmonary Medicine, Cancer Hospital of Xinjiang Medical University, 789 Suzhou Street, Urumqi, 830011, Xinjiang, China

ARTICLE INFO

Keywords:
Non-small cell lung cancer
Costimulatory molecule
Prognosis
Immunotherapy

ABSTRACT

Background: Non-small cell lung cancer (NSCLC) is a leading cause of cancer-related mortality worldwide. Despite advances in treatment, prognosis remains poor, necessitating the identification of reliable prognostic biomarkers. Costimulatory molecules (CMs) have shown to enhance antitumor immune responses. We aimed to explore their prognostic signals in NSCLC.

Methods: This study is a combination of bioinformatics analysis and laboratory validation. Gene expression profiles from The Cancer Genome Atlas (TCGA), GSE120622, and GSE131907 datasets were collected. NSCLC samples in TCGA were clustered based on CMs using consensus clustering. We used LASSO regression to identify CMs-related signatures and constructed nomogram and risk models. Differences in immune cells and checkpoint expressions between risk models were evaluated. Enrichment analysis was performed for differentially expressed CMs between NSCLC and controls. Key results were validated using qRT-PCR and flow cytometry.

Results: NSCLC samples in TCGA were divided into two clusters based on CMs, with cluster 1 showing poor overall survival. Ten CMs-related signatures were identified using LASSO regression. NSCLC samples in TCGA were stratified into high- and low-risk groups based on the median risk score of these signatures, revealing differences in survival probability, drug sensitivity, immune cell infiltration and checkpoints expression. The area under the ROC curve values (AUC) for EDA, ICOS, PDCD1LG2, and VTCN1 exceeded 0.7 in both datasets and considered as hub genes. Expression of these hub genes was significance in GSE131907 and validated by qRT-PCR. Macrophage M1 and T cell follicular helper showed high correlation with hub genes and were lower in NSCLC than controls detected by flow cytometry.

Conclusion: The identified hub genes can serve as prognostic biomarkers for NSCLC, aiding in treatment decisions and highlighting potential targets for immunotherapy. This study provides new insights into the role of CMs in NSCLC prognosis and suggests future directions for clinical research and therapeutic strategies.

1. Introduction

Lung cancer is the leading cause of cancer-related death worldwide [1], with non-small cell lung cancer (NSCLC) accounting for 85 % of all cases. Despite efforts to improve early diagnosis of NSCLC, most patients are usually diagnosed at advanced stages of the disease [2], the 5-year overall survival (OS) rate remains only 16 % [3]. Current treatments include surgery, chemotherapy, molecular

* Corresponding author.
E-mail address: 2001xiaogu@163.com (G. Gu).

https://doi.org/10.1016/j.heliyon.2024.e36816
Received 6 March 2024; Received in revised form 21 August 2024; Accepted 22 August 2024
Available online 30 August 2024

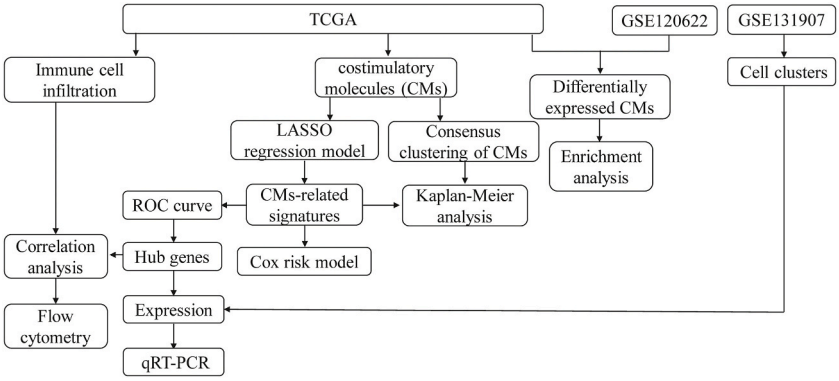

Fig. 1. The flowchart of this study.

targeted therapy and radiation [4], but high recurrence, metastasis, adverse effects, and drug resistance persist make the 5-year OS rate of patients still unsatisfactory. Therefore, new therapeutic strategies are urgently needed to complement traditional chemotherapy.

Recently, immunotherapy has dramatically changed the therapeutic landscape of NSCLC, with immune checkpoint inhibitors (ICI) improving clinical outcomes by targeting cancer cells to evade the immune system [5,6]. Studies have shown that a deeper understanding of the immune microenvironment will help us improve the prognosis of patients with NSCLC [7]. Many studies are currently exploring the therapeutic potential of costimulatory molecules (CMs) in cancer [8]. CMs have been shown to enhance antitumor immune responses [9]. CMs play an important role in tumor immune regulation by influencing T cell activation, proliferation, and survival [10]. Although their roles in NSCLC are not well understood, CMs may provide valuable prognostic information and therapeutic targets. In addition, the diagnosis of NSCLC and the recognition of its subtypes are also prognostic and predictive factors. Targeted therapy based on genotyping has also emerged as one of the therapeutic approaches for NSCLC [11].

Studies have explored the prognostic value of CMs [12,13]. However, these studies did not fully elucidate the molecular functions of CMs in NSCLC or their potential in guiding treatment strategies. Our study aims to fill these gaps by evaluating the prognostic role of CMs in NSCLC and developing effective prognostic signals to guide treatment and improve clinical outcomes. We selected TCGA and GSE120622 datasets and performed various bioinformatics analyses to evaluate the prognostic role of CMs in NSCLC. Aimed to elucidate the mechanisms underlying the effects of CMs and develop an effective prognostic signal based on multiple CMs to guide treatment and improve clinical outcomes in NSCLC.

2. Materials and methods

2.1. Study design

This study comprises two main phases: bioinformatics analysis and laboratory validation, as shown in Fig. 1.

2.2. Data collection

The normalized gene expression dataset from The Cancer Genome Atlas (TCGA; https://www.cancer.gov/tcga) included 1019 NSCLC samples and 110 normal controls. GSE120622 and GSE131907 datasets were collected from Gene Expression Omnibus database (GEO; https://www.ncbi.nlm.nih.gov/gds). GSE120622 dataset included gene expression profiles of NSCLC patients by high throughput sequencing based on GPL20301 platform, which included 81 lung cancer tissues and 19 adjacent lung tissues. The expression levels of CMs were collected from both datasets. Patients' overall survival information was taken from the TCGA and GSE120622 datasets. GSE131907 dataset including single cell RNA sequencing (scRNA-seq) for 15 lung adenocarcinomas and 11 normal lung tissues separated from the malignant region by at least 5 cm.

2.3. Consensus clustering of CMs

To identify the prognostic values of CMs, we clustered NSCLC samples from TCGA into different clusters employing ConsensusClusterPlus package [14]. Kaplan-Meier (K-M) survival analysis was performed to compare the different OS between different clusters.

2.4. Prognostic signature construction

To further selected useful prognostic signatures, the CMs were analyzed using least absolute shrinkage and selector operation (LASSO) regression model by glmnet package [15]. The optimal λ was chosen to yield minimum cross validation error in 10-fold cross validation. The top 10 regression coefficients were selected as CMs-related signatures. Next, the nomogram and calibration curves

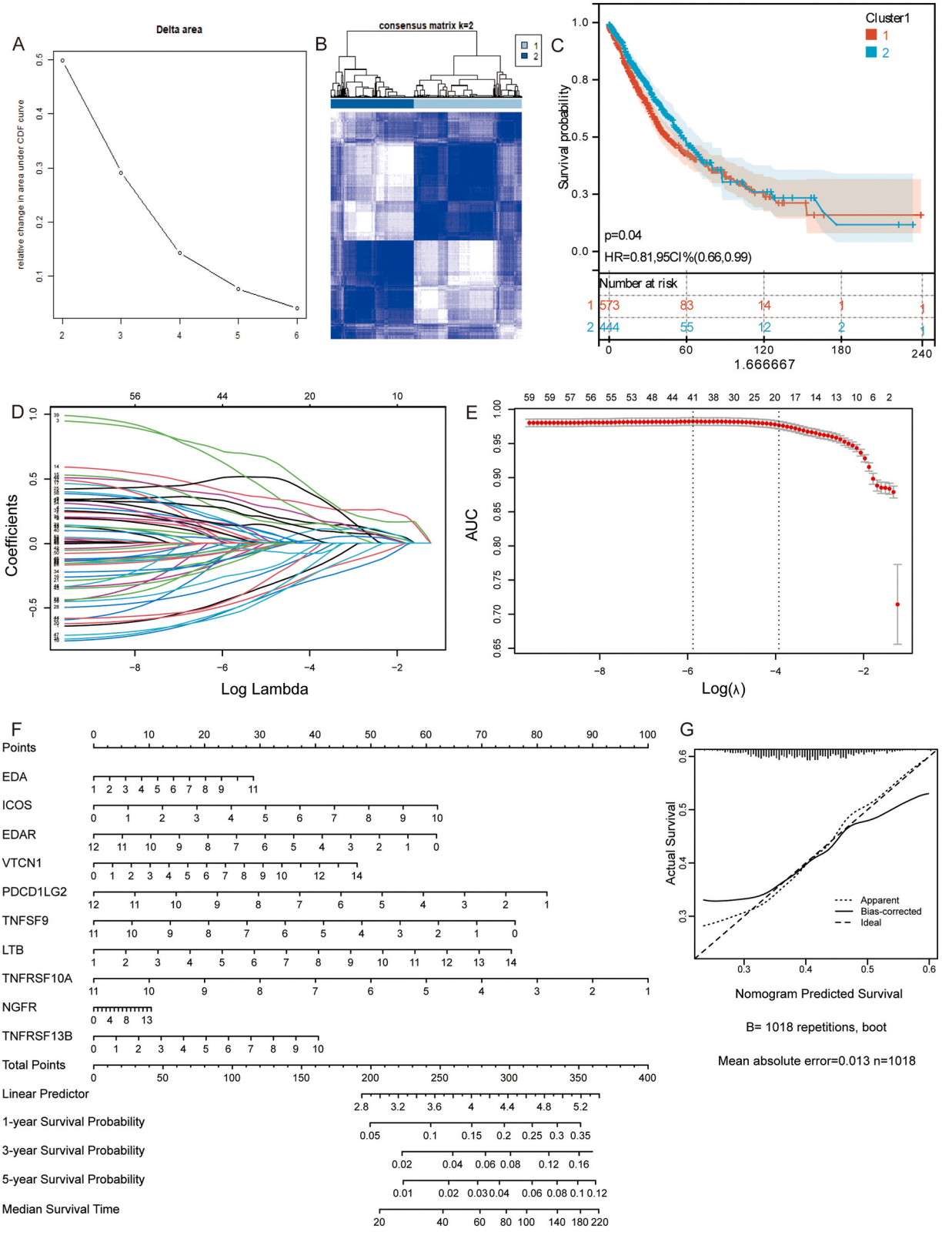

(caption on next page)

Fig. 2. Construction of prognostic model in NSCLC based on costimulatory molecules. (A) The relative change in area under the cumulative distribution function (CDF) curve for k = 2. (B) Consensus clustering matrix for k = 2. (C) Kaplan–Meier curves for overall survival (OS) of cluser1 and cluster 2. (D) Distribution of LASSO coefficients for costimulatory molecules. (E) Confidence interval in every lambda of LASSO regression. (F) Nomogram of CMs-related signatures for 1-, 3- and 5-year OS of NSCLC. (G) Calibration curve for OS of NSCLC patients in nomogram-predicted and ideal model.

were created using rms package in the TCGA based on CMs-related signatures.

According to the CMs-related signatures, the risk score was calculated using Cox regression analysis. Then NSCLC samples from TCGA was divided into low-and high-risk groups according to the median of the risk score. Genomics of Drug Sensitivity in Cancer (GDSC) [16] was used to predict the sensitivity to common anticancer drugs for samples in low-and high-risk groups.

2.5. Survival analysis of CMs in NSCLC

The receiver operating characteristic (ROC) curve was performed using pROC package to assess the sensitivity and specificity of CMs-related signatures. K-M survival analysis was performed in both datasets to further elucidate the prognostic significance of CMs-related signatures in NSCLC patients.

2.6. Infiltration of immune cells

The immune landscape for 22 types of tumor-infiltrating immune cells between the high- and low-risk groups were inferred using CIBERSORT algorithm [17]. The immuneScore, stromalScore, and ESTIMATEScore between the high- and low-risk groups were calculated using ESTIMATE algorithm. A $P < 0.05$ was considered statistically significant. Correlations analyses were calculated using Pearson correlation analysis.

2.7. Data processing on scRNA-seq

Fastq files from GSE131907 were collected and performed unique molecular identifier processing. Low-quality cells with mitochondrial genes $\leq$20 %, UMI $\leq$200, and gene count $\geq$6000 were excluded. The top 2000 highest variance genes were used for downstream analysis. Uniform Manifold Approximation and Projection (UMAP) was used to further reduce dimensionality for easier visualization and interpretation of data. Cell clusters were annotated based on previously published articles.

2.8. Differential analysis and enrichment analysis

Differential analysis between NSCLC and controls in TCGA and GSE120622 were analyzed using DESeq2 package [18]. The results with adj P value < 0.05 was set as the cutoff value to obtain differentially expressed genes (DEGs). The overlap genes of DEGs in both datasets and CMs were obtained by intersection analysis.

Enrichment analysis of Gene Ontology (GO) and Kyoto Encyclopedia of Genes and Genomes (KEGG) pathway for overlap genes were performed using ClusterProfiler package in R [19]. A P value < 0.05 was considered statistically significant.

2.9. Sample collection

The lung cancer tissues and adjacent healthy lung tissues from 10 NSCLC patients, as well as peripheral blood samples of 10 NSCLC patients and 10 normal controls were collected from Cancer Hospital of Xinjiang Medical University. This study was approved by the Ethics Committee of Cancer Hospital of Xinjiang Medical University (No. K-2022016). Informed consent was known and signed by all participants.

2.10. Quantitative real-time PCR (qRT-PCR)

Total RNA was extracted from lung cancer tissues and adjacent healthy lung tissues using Trizol (Invitrogen, CA, USA). The cDNA was synthesized using total RNA with Primescript RT master mixture (Invitrogen). The qRT-PCR reaction was performed using SYBR Green PCR master mix (Invitrogen). The specific primer sequences were shown in Table S1. The relative mRNA level of genes was normalized to GAPDH based on $2^{-\Delta\Delta Ct}$ method.

2.11. Flow cytometry

The abundances of Macrophage M1, and T cell follicular helper were detected in peripheral blood samples using flow cytometry. For analysis of cell surface markers, the cells were stained with anti-human CD68 PC7, anti-human CD86 FITC, anti-human CD4-FITC, anti-human CXCR5-PE (BD Biosciences, CA, USA). Blood samples and red blood cell lysates (BD Biosciences) were co-incubated for 10 min and then washed three times with PBS. The assay data were analyzed using FlowJo software.

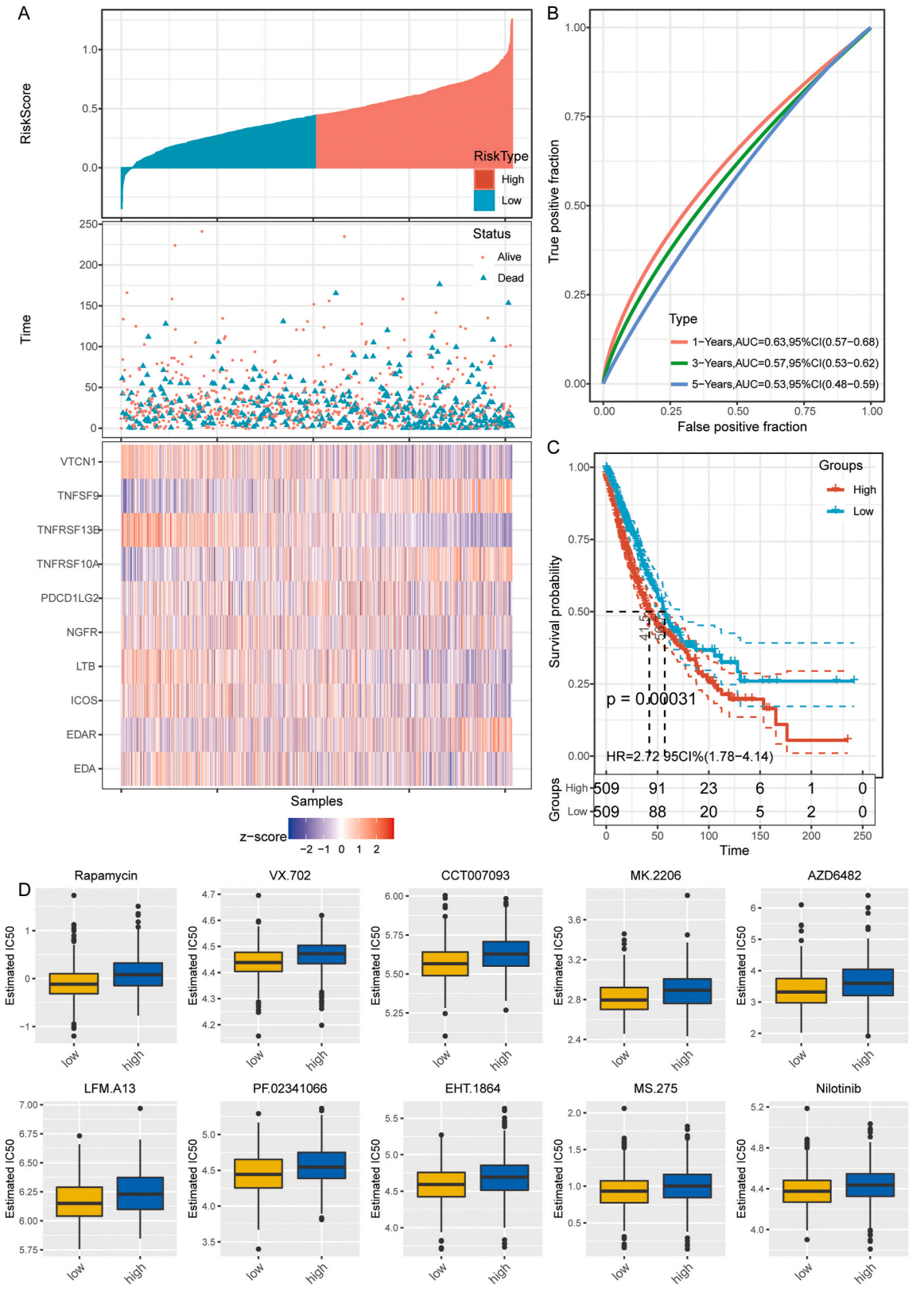

(caption on next page)

Fig. 3. Risk score model analysis of NSCLC based on CMs-related signatures in TCGA. (A) Distribution of patient overall survival and gene expression levels based on median risk score. (B) AUCs of median risk score for prediction of overall survival in 1-, 3-, and 5-year. (C) The K–M curve of high- and low-risk groups. (D) The estimated IC_{50} for predicted significantly different sensitivity drugs in high- and low-risk groups.

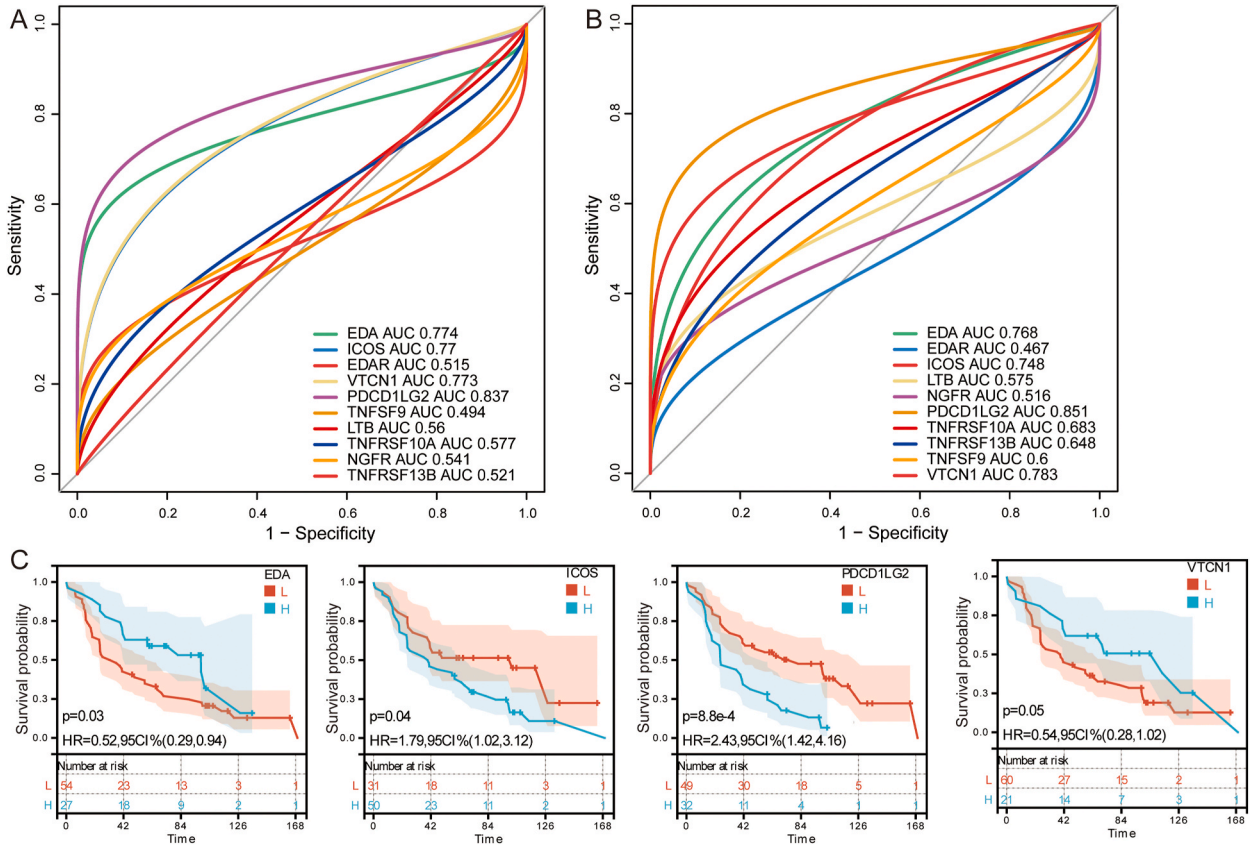

Fig. 4. Identification of hub genes. ROC curves of CMs-related signatures in TCGA (A) and GSE120622 (B) datasets. (C) K–M curve of hub genes.

2.12. Statistical analysis

All statistical analyses were performed using the R 4.0.1 or GraphPad Prism 6.0 software. Multiple testing corrections were applied to control for false discovery rates. Comparison between groups was performed using Student's *t*-test. A P values < 0.05 were considered statistically significant.

3. Results

3.1. Prognostic model of costimulatory molecules in NSCLC

To evaluate the prognostic role of CMs in patients, we utilized consensus clustering to split patients into two clusters (Fig. 2A and B). NSCLC patients in cluster 1 showed significantly poorer OS than that in cluster 2 (Fig. 2C). Using LASSO regression analysis, we identified 10 regression coefficients as CMs-related signatures (Fig. 2D and E).

We constructed a nomogram to predict the OS rates for NSCLC patients based on CMs-related signatures (Fig. 2F). Each factor had a certain score in the nomogram. It potentially more clinically useful for predicting OS in NSCLC patients. Calibration plots showed that the nomogram performed well compared with an ideal model (Fig. 2G).

3.2. Construction of risk score model and identification of hub genes

NSCLC patients in TCGA were stratified into high- and low-risk groups based on median risk score of the CMs-related signatures (Fig. 3A). The area under the ROC curve (AUC) value was 0.63 for 1-year OS, 0.57 for 3-year OS, and 0.53 for 5-year OS according to median risk score (Fig. 3B). Then the patients in the high-risk group showed poor survival probability (Fig. 3C). To further explore

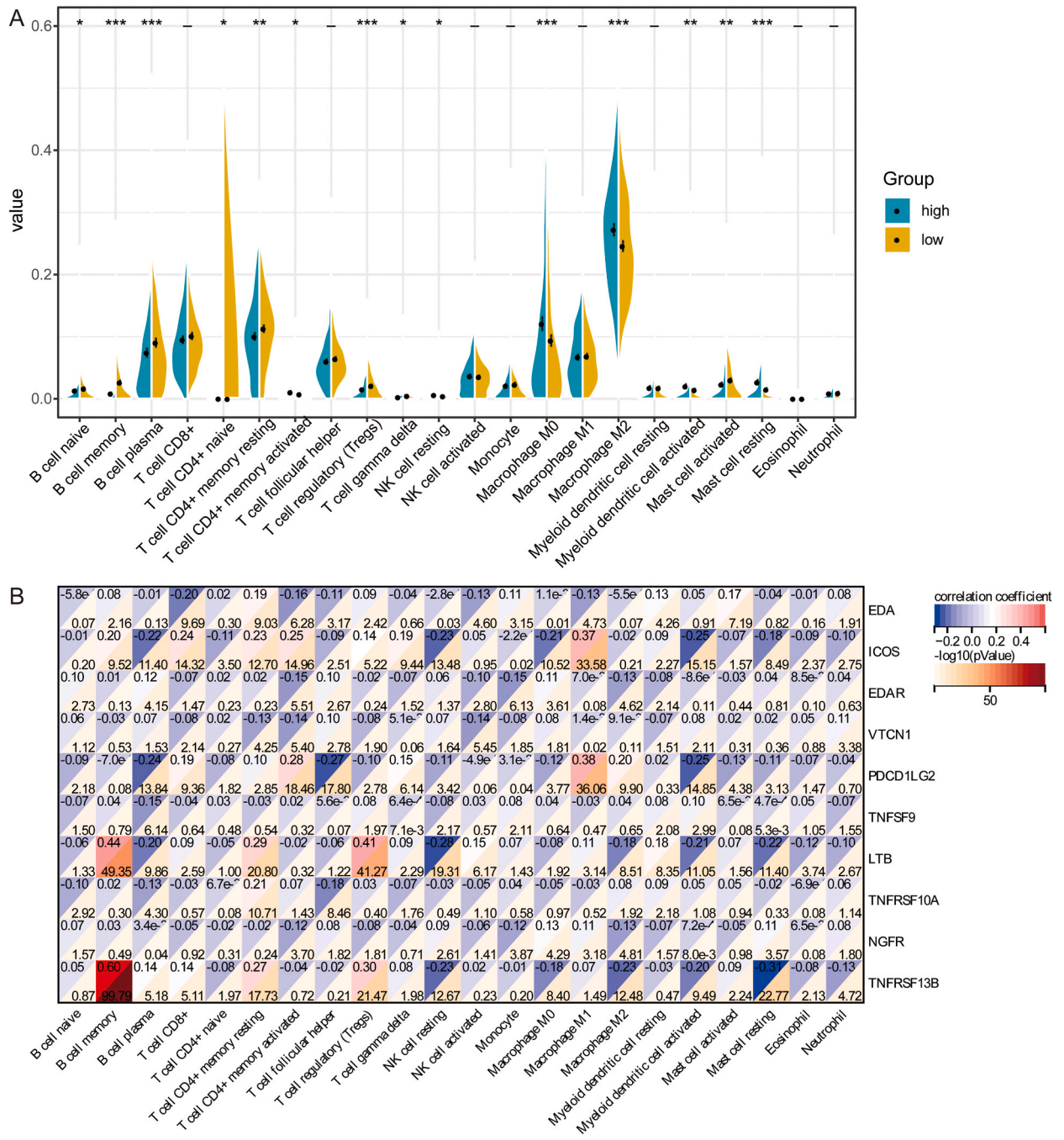

Fig. 5. Immune cell abundance between high- and low-risk groups. (A) Different immune cell infiltration levels between high- and low-risk groups in TCGA. $^{*}P < 0.05$, $^{**}P < 0.01$, $^{***}P < 0.001$. (B) Correlation between infiltration levels of immune cells and expression of CMs-related signatures.

differences of drug sensitivity between high- and low-risk groups, we trained a model with data from GDSC cells to predict IC_{50} for common chemotherapy drugs. We predicted that Rapamycin, VX.702, CCT007093, MK.2206, AZD6482, LFM.A13, PF.02341066, EHT.1864, MS.275, and Nilotinib were significantly different sensitivity in high- and low-risk groups (Fig. 3D).

To further identify hub genes in CMs-related signatures, we calculated AUC values in TCGA (Fig. 4A) and GSE120622 (Fig. 4B) datasets. AUC values for EDA, ICOS, PDCD1LG2, and VTCN1 were all greater than 0.7 in both datasets and considered as hub genes. Survival analysis results showed that highly expressed ICOS, and PDCD1LG2 showed poorer prognosis (Fig. 4C).

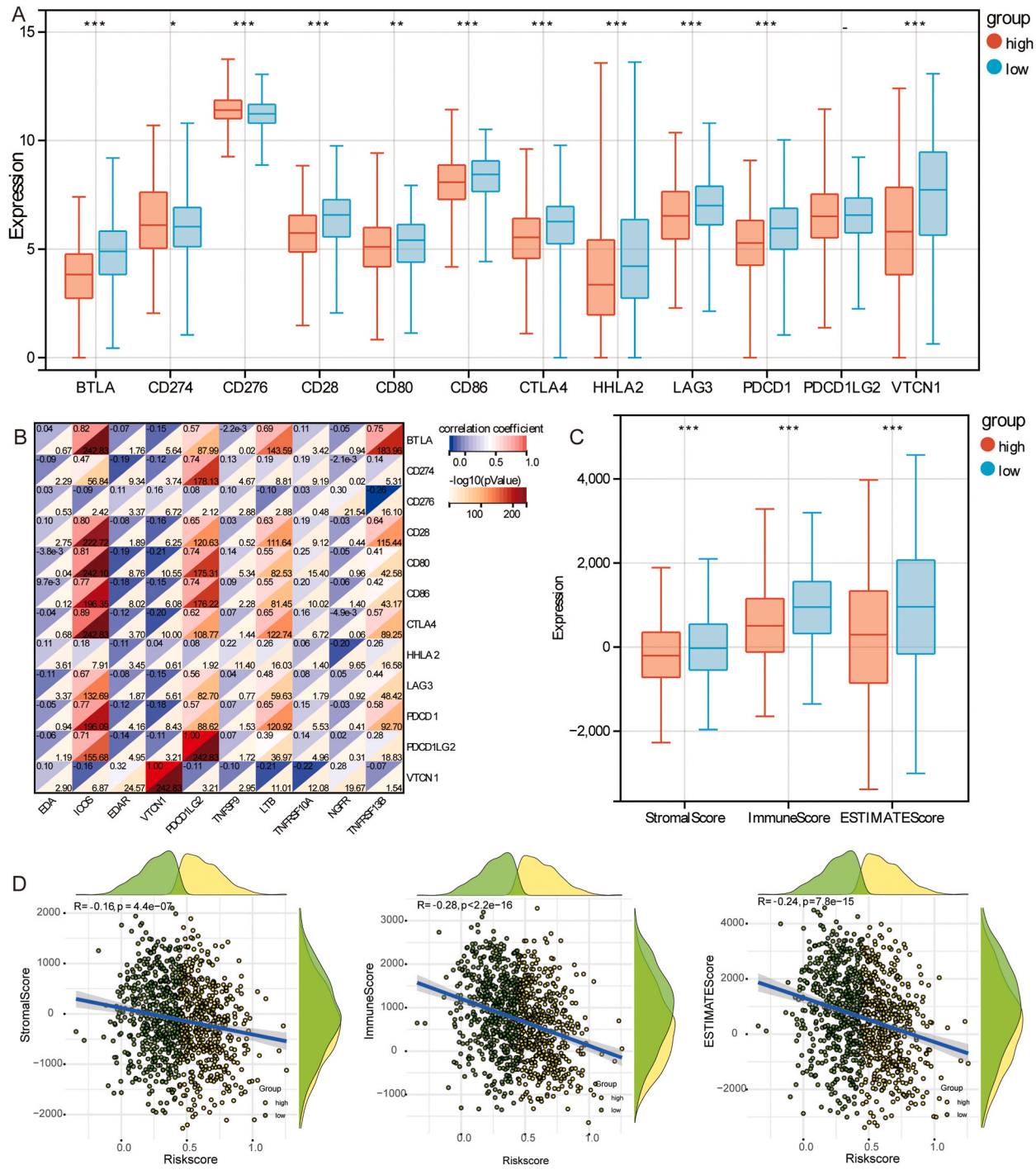

Fig. 6. Evaluation of immune check points and immune microenvironment in TCGA. (A) Different expression of immune check points between high- and low-risk groups. (B) Correlation between immune check points and CMs-related signatures. (C) Different expression of immuneScore, stromalScore, and ESTIMATEScore between high- and low-risk groups. (D) Correlation between median risk score and immuneScore, stromalScore, or ESTIMATEScore. $^{*}P < 0.05$, $^{**}P < 0.01$, $^{***}P < 0.001$.

3.3. Different immune microenvironment between high- and low-risk groups

We investigated the different infiltration levels of immune cell types between high- and low-risk groups in TCGA (Fig. 5A). The proportion of T cell $CD4^{+}$ memory activated, macrophage M0, macrophage M2, myeloid dendritic cell activated, and mast cell resting

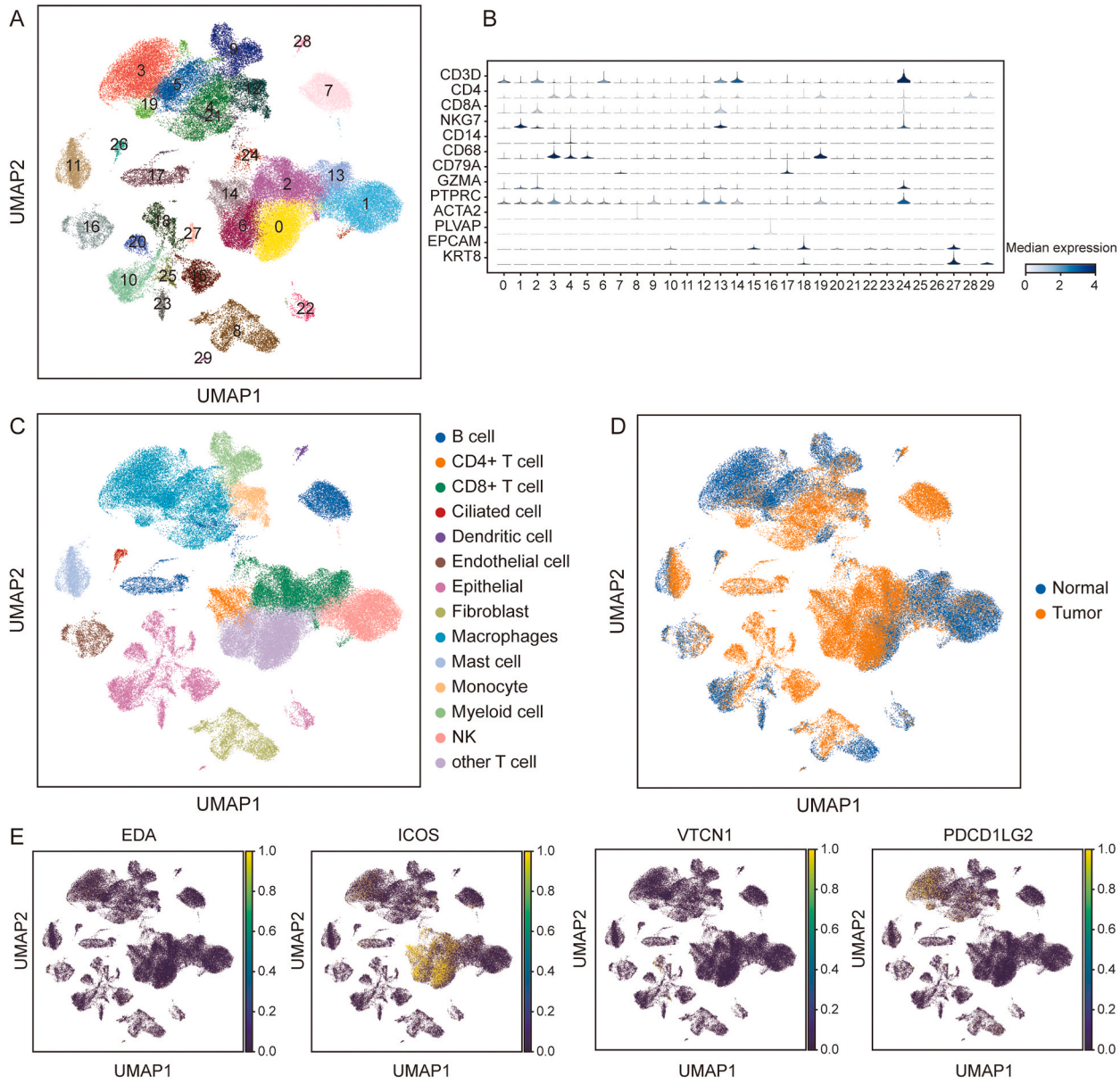

Fig. 7. Expression of hub genes in cells by scRNA-seq. (A) UMAP plot of all cells with identified into 29 cell clusters. (B) Expression of main cell markers in cell clusters (C) UMAP plot of 14 cell subpopulations, color-coded by corresponding cell type. (D) UMAP plot of all cells in different groups. (E) UMAP plot of expression of hub genes in cell clusters in different groups.

were all higher in the high-risk group than low-risk group. B cell naïve, B cell memory, B cell plasma, T cell CD4$^+$ naïve, T cell CD4$^+$ memory resting, T cell regulatory (Tregs), T cell gamma delta, NK cell resting, and mast cell activated were all lower in high-risk group. We also calculated the correlation between immune cells and CMs-related signatures (Fig. 5B). Results showed that macrophage M1 and ICOS or PDCD1LG2 had the higher positive correlation, T cell follicular helper (Tfh) and PDCD1LG2 had negative correlation.

In addition, we compared the differences in immune check points expression between high- and low-risk groups (Fig. 6A). In addition to CD274 and CD276, other check points were all lower expression in high-risk group. Fig. 6B showed the relation among check points and CMs-related signatures. ICOS was positively associated with most check points, while VTCN1 was negatively associated with most check points. Interestingly, immuneScore, stromalScore, and ESTIMATEScore were all lower in the high-risk group than low-risk group (Fig. 6C). Correlation analysis results showed immuneScore, stromalScore, and ESTIMATEScore were negatively related with median risk score (Fig. 6D).

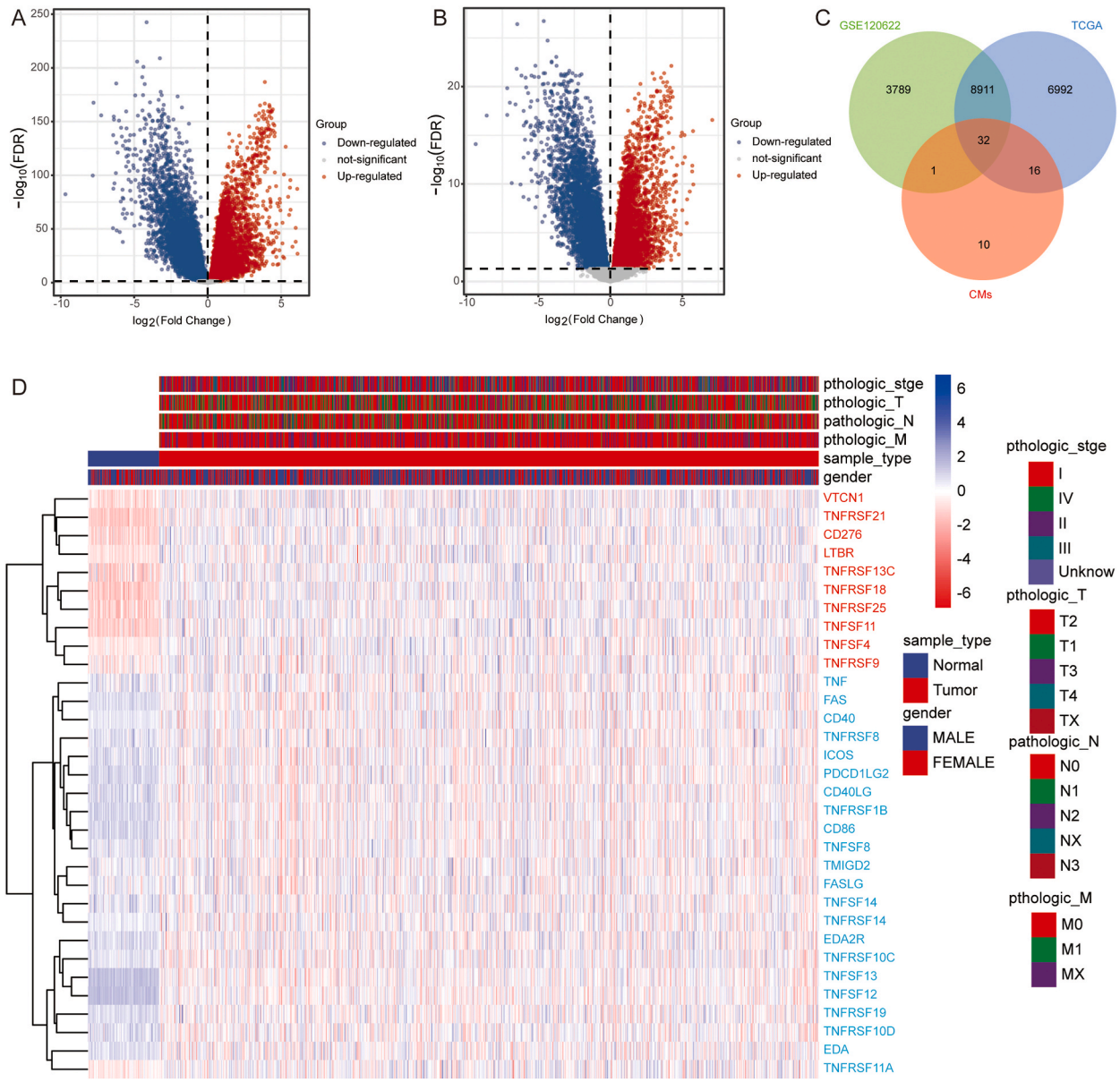

Fig. 8. Identification of differentially expressed CMs. Differentially expressed genes between NSCLC and controls in TCGA (A) and GSE120622 (B) datasets. (C) Overlap of differentially expressed genes and CMs were differentially expressed CMs. (D) Heatmap of differentially expressed CMs in TCGA. Red is upregulated expression and blue is downregulated expression in NSCLC.

3.4. Expression of hub genes in single cell

In the UMAP of scRNA-seq, we identified 29 cell clusters (Fig. 7A). We annotated cell clusters as 14 major cell subpopulations based on the expression of cell markers (Fig. 7B and C). which including B cells, $CD4^+$ T cells, $CD8^+$ T cells, ciliated cells, dendritic cells, endothelial cells, epithelial, fibroblast, macrophages, mast cells, monocyte, myeloid cells, NK cells, and other T cells. NK cells were mainly enriched in normal tissues, B cells were mainly enriched in tumor tissues (Fig. 7D). Accordingly, ICOS was mainly expressed in $CD4^+$ T cells, $CD8^+$ T cells, and other T cells in tumor tissues, PDCD1LG2 was mainly expressed in macrophages in normal tissues (Fig. 7E).

3.5. Differentially expressed CMs and biological functions

To identify the differentially expressed CMs, we first analyzed the DEGs in TCGA and GSE120622 datasets. There were 15951 DEGs in the TCGA (Fig. 8A) and 12733 DEGs in the GSE120622 (Fig. 8B). Finally we found 32 differentially expressed CMs (Fig. 8C and D).

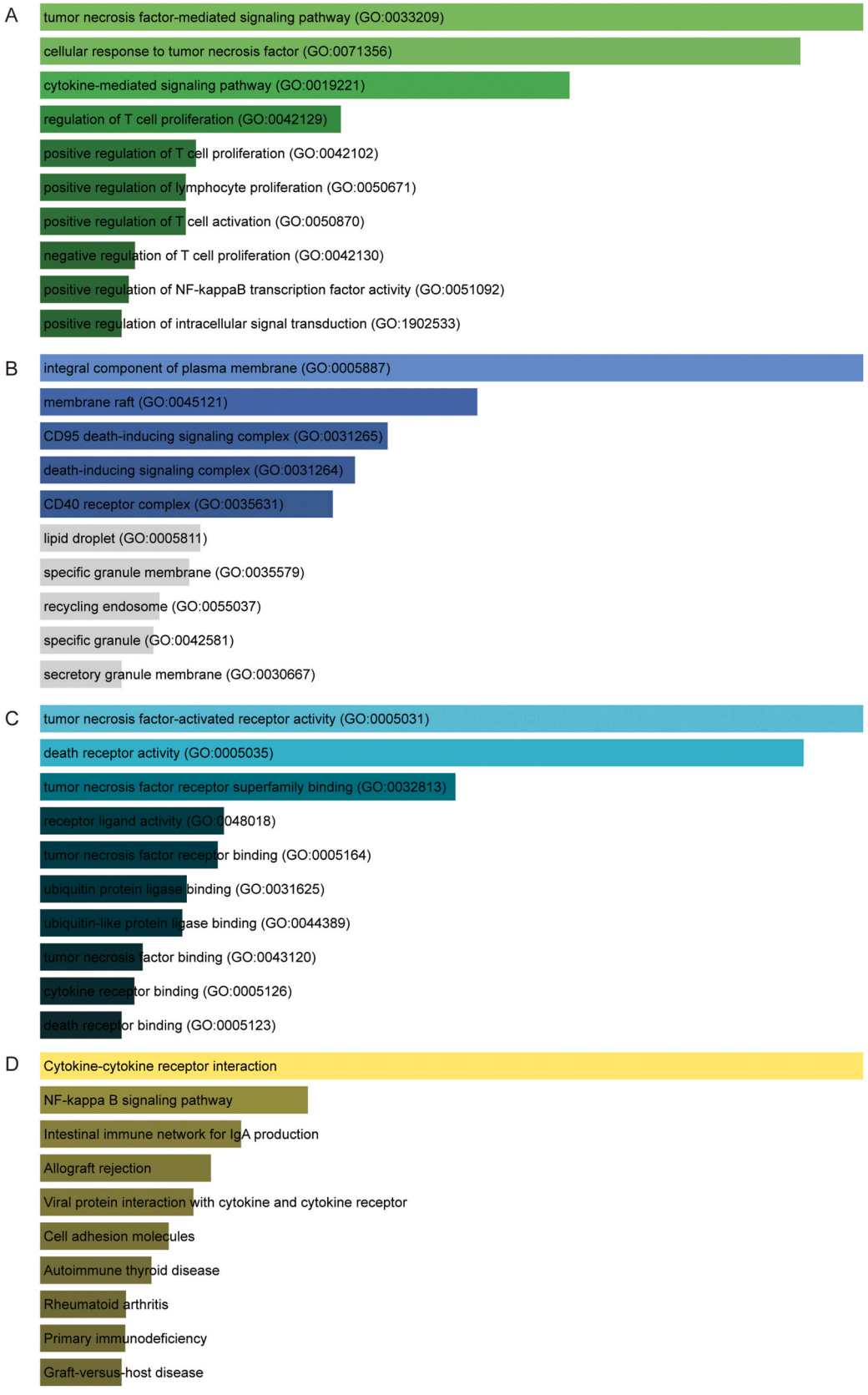

(caption on next page)

Fig. 9. Enrichment analysis for differentially expressed CMs. Enrichment of biological process (A), cellular component (B), and molecular function (C) for differentially expressed CMs. (D) KEGG pathways of differentially expressed CMs mainly enriched.

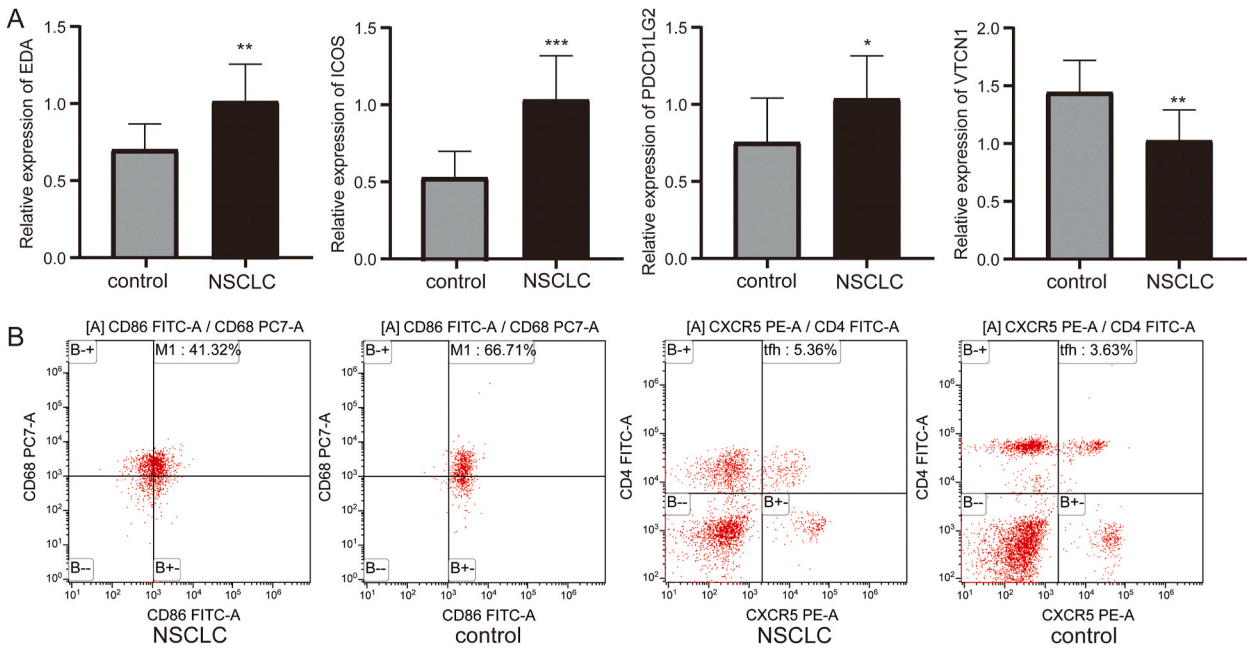

Fig. 10. Laboratory validation of key results. (A) Relative mRNA levels of EDA, ICOS, PDCD1LG2, and VTCN1 in cancer and healthy normal tissue detected by qRT-PCR. (B) Different infiltration levels of macrophage M1 and Tfh in NSCLC and controls detected by flow cytometry. $^{*}P < 0.05$, $^{**}P < 0.01$, $^{***}P < 0.001$.

Enrichment results showed that differentially expressed CMs were mainly enriched in tumor necrosis factor (TNF)-mediated signaling pathway, cellular response to TNF, and regulation of T cell proliferation of biological process (Fig. 9A). For cellular component, integral component of plasma membrane, membrane raft, and CD95 death-inducing signaling complex were involved (Fig. 9B). Then, TNF-activated receptor activity, death receptor activity, and TNF receptor superfamily binding were the main molecular function results (Fig. 9C). In the KEGG pathways, we found that Cytokine-cytokine receptor interaction, NF-kappa B signaling pathway, and intestinal immune network for IgA production were significantly enriched by differentially expressed CMs (Fig. 9D).

3.6. Laboratory validation

Moreover, cancer lung tissue and adjacent healthy controls samples of NSCLC were used to validate the expression of hub genes by qRT-PCR method (Fig. 10A). EDA, ICOS, and PDCD1LG2 were higher expression, and VTCN1 were lower expression in cancer samples than that in controls.

Importantly, the abundance of macrophage M1 and Tfh between NSCLC and controls was examined using flow cytometry (Fig. 10B). The abundances of macrophage M1 were lower in NSCLC than controls, and Tfh cells were higher.

4. Discussion

Despite advances in treatment, NSCLC prognosis remains poor. Studies have reported immune related genes as prognostic indicators in NSCLC [20]. In recent years, immunotherapy has been applied to the treatment of NSCLC. Immunotherapy is safer and more effective than conventional treatments and provides better guidance for the clinical management of patients with advanced NSCLC [21]. Previous studies have revealed the involvement of CMs in the progression of various tumors, playing an important role in tumor immune regulation [22,23], and understanding CMs' roles can enhance treatment strategies.

To improve the clinical treatment outcome of NSCLC, we identified four CMs and constructed a prognostic risk model for NSCLC patients based on them. To our knowledge, our study is the first to describe a prognostic model for CMs in patients with NSCLC. Importantly, we validated the aberrant expression of the four CMs in NSCLC patients in clinical samples. In addition, we also analyzed the correlation between CMs and immune cells and verified the abundance of important immune cells. These results suggested that the four CMs might affect the prognosis of NSCLC patients by modulating the immune microenvironment.

In the four CMs genes with prognostic diagnostic value (EDA, ICOS, PDCD1LG2, and VTCN1), ectodysplasin A (EDA), a member of the tumor necrosis factor superfamily, regulates ectodermal development in various organs [24]. EDA gene expression contributes to the maintenance of epithelial barrier function [25]. EDA was downregulated in cervical cancer [26]. EDA receptor regulate

Wnt/β-catenin signaling pathway promotes colorectal cancer cell proliferation [27]. EDA receptor signalling in NSCLC has received little attention, despite it effected NFκB signalling, which associated with NSCLC [28,29]. Inducible T cell costimulator (ICOS; CD278) may serve as a potential therapeutic target for anticancer therapy [30]. However, the expression of ICOS in NSCLC was significantly associated with improved OS in a study by Monkman et al. [31]. The programmed cell death 1 ligand 2 (PDCD1LG2; PD-L2) may be highly expressed as a result of cancer cell autonomous mechanisms, leading to intrinsic immune resistance [32]. High PD-L1 and PDCD1LG2 coexpression levels are associated with worse OS in NSCLC patients [33]. V-set domain containing T cell activation inhibitor 1 (VTCN1; B7-H4) induces NSCLC immune escape by upregulating the PD-1/STAT3 pathway [34]. Knockdown of VTCN1 significantly reduced apoptosis and promoted T cell-mediated antitumor immunity in A549 cells [35]. Although VTCN1 is associated with tumor infiltrating lymphoycte, its expression does not always correlate with survival [36].

Through scRNA seq analysis, cell heterogeneity in the tumor microenvironment (TME) was successfully depicted, emphasizing the crucial role of different cell types in tumor development and immune response in TME [37]. In particular, the discovery of B cell enrichment in tumor tissue supports the dual role that B cells may play in tumor immunity, promoting immune responses by producing antibodies and presenting antigens, as well as contributing to tumor immune escape by regulating T cell function and promoting the formation of an inflammatory environment [38]. The observation that NK cells are mainly enriched in normal tissues suggests that the anti-tumor activity of NK cells may be more critical in the early stages of tumor development, and their function may be inhibited in the tumor microenvironment. This is consistent with the role of NK cells in immune surveillance and their importance in early recognition and clearance of tumor cells [39].

The results of correlation analysis suggested that macrophage M1 and Tfh had the highest correlation with PDCD1LG2. In diffuse large B-cell lymphoma, the expression level of PDCD1LG2 is positively correlated with the expression status of the macrophage M1 marker CD86 [40]. PDCD1LG2 expression on B cells decreased the number of Tfh cells, controls formation of long live plasma cells [41]. However, whether PDCD1LG2 regulates the functions and roles of macrophage M1 and Tfh in NSCLC remains unclear.

Moreover, CMs differentially expressed in NSCLC were significantly enriched in TNF related signaling pathways. TNFs play a key role in antitumor immune responses [42]. Many immune cells secrete TNF-α and then plays a role in cancer [43], Higher levels of TNF-α in serum of NSCLC patients may have positive prognostic value [44]. However, TNF-α is considered a cytokine with dual roles in cancer progression. Constitutive expression of TNF-α in the inflammatory tumor microenvironment plays a pro tumorigenic role by enhancing cancer cell survival, angiogenesis, and metastasis formation and is associated with poor prognosis in patients with NSCLC [45,46]. Therefore, targeted regulation of the TNF related signaling pathway may have great implications for the treatment of NSCLC.

CMs are emerging as significant players in the field of cancer immunotherapy. Their ability to modulate immune responses makes them promising targets for developing new therapeutic strategies. In clinical practice, CMs have shown potential in enhancing the efficacy of existing treatments, particularly immune checkpoint inhibitors [47,48]. The current situation in clinical practice and research underscores the need for reliable prognostic biomarkers and effective immunotherapeutic strategies. Our findings contribute to this by providing new insights into the prognostic roles of CMs and their potential as therapeutic targets.

Our study has limitations. The main data source of this study was public databases, and the prognostic information of NSCLC patients was limited, further validation in larger clinical cohorts is needed. The prognostic diagnostic role of the 4 CMs needs to be verified in a large number of clinical samples. Second, the content of this study was CMs, without comprehensive understanding of the tumor immune microenvironment, resulting in limited predictive power of genes. Furthermore, the ability of CMs-related signatures to respond to immunotherapy is unclear. Further studies on NSCLC patients undergoing immunotherapy are needed to confirm the clinical utility of our four CMs.

5. Conclusion

This study identified distinct immune infiltration patterns in NSCLC risk models based on CMs-related signatures. Four CMs (EDA, ICOS, PDCD1LG2, and VTCN1) were identified as reliable prognostic biomarkers associated with the immune microenvironment. These findings advance the development of immunotherapeutic strategies for NSCLC patients by providing new targets for enhancing antitumor immune responses. Moreover, our results suggest that incorporating CMs into risk stratification models can improve the accuracy of prognostic predictions and guide personalized treatment decisions.

Funding

This study was supported by the grants from the Natural Science Foundation of Xinjiang Uygur Autonomous Region (2021D01C381; 2022D01C796).

Data availability statement

The data used to support the findings of this study are available from The Cancer Genome Atlas (TCGA), GSE120622 and GSE131907 datasets.

Ethics approval and consent to participate

All experimental protocols conformed to the World Medical Association Declaration of Helsinki and were approved by the Ethics Committee of Cancer Hospital of Xinjiang Medical University (No. K-2022016), and all the patients signed written informed consent.

CRediT authorship contribution statement

Yan Yang: Writing – original draft, Investigation. **Suqiong Lu:** Software, Methodology, Formal analysis. **Guomin Gu:** Writing – review & editing, Funding acquisition.

Declaration of competing interest

The authors declare the following financial interests/personal relationships which may be considered as potential competing interests:No reports was provided by No. No reports a relationship with No that includes:. No has patent pending to No. No If there are other authors, they declare that they have no known competing financial interests or personal relationships that could have appeared to influence the work reported in this paper.

Acknowledgments

Not applicable.

Appendix A. Supplementary data

Supplementary data to this article can be found online at https://doi.org/10.1016/j.heliyon.2024.e36816.

References

[1] R.L. Siegel, K.D. Miller, H.E. Fuchs, A. Jemal, Cancer statistics, CA Cancer J Clin 72 (1) (2022) 7–33.
[2] J. Kapeleris, M. Ebrahimi Warkiani, A. Kulasinghe, I. Vela, L. Kenny, R. Ladwa, K. O'Byrne, C. Punyadeera, Clinical applications of circulating tumour cells and circulating tumour DNA in non-small cell lung cancer-an update, Front. Oncol. 12 (2022) 859152.
[3] M. Alam, S. Alam, A. Shamsi, M. Adnan, A.M. Elasbali, W.A. Al-Soud, M. Alreshidi, Y.M. Hawsawi, A. Tippana, V.R. Pasupuleti, M.I. Hassan, Bax/Bcl-2 cascade is regulated by the EGFR pathway: therapeutic targeting of non-small cell lung cancer, Front. Oncol. 12 (2022) 869672.
[4] J. Peinado-Serrano, A. Carnero, Molecular radiobiology in non-small cell lung cancer: prognostic and predictive response factors, Cancers 14 (9) (2022).
[5] O. Rodak, M.D. Peris-Diaz, M. Olbromski, M. Podhorska-Okolow, P. Dziegiel, Current landscape of non-small cell lung cancer: epidemiology, histological classification, targeted therapies, and immunotherapy, Cancers 13 (18) (2021).
[6] T. Cascone, J. Fradette, M. Pradhan, D.L. Gibbons, Tumor immunology and immunotherapy of non-small-cell lung cancer, Cold Spring Harb Perspect Med 12 (5) (2022).
[7] J. Kang, C. Zhang, W.Z. Zhong, Neoadjuvant immunotherapy for non-small cell lung cancer: state of the art, Cancer Commun. 41 (4) (2021) 287–302.
[8] X. Hua, S. Ge, J. Zhang, H. Xiao, S. Tai, C. Yang, L. Zhang, C. Liang, A costimulatory molecule-related signature in regard to evaluation of prognosis and immune features for clear cell renal cell carcinoma, Cell Death Discov 7 (1) (2021) 252.
[9] N. Aschmoneit, K. Kocher, M. Siegemund, M.S. Lutz, L. Kuhl, O. Seifert, R.E. Kontermann, Fc-based Duokines: dual-acting costimulatory molecules comprising TNFSF ligands in the single-chain format fused to a heterodimerizing Fc (scDk-Fc), OncoImmunology 11 (1) (2022) 2028961.
[10] S. Ge, X. Hua, J. Chen, H. Xiao, L. Zhang, J. Zhou, C. Liang, S. Tai, Identification of a costimulatory molecule-related signature for predicting prognostic risk in prostate cancer, Front. Genet. 12 (2021) 666300.
[11] C. Aggarwal, C.D. Rolfo, G.R. Oxnard, J.E. Gray, L.M. Sholl, D.R. Gandara, Strategies for the successful implementation of plasma-based NSCLC genotyping in clinical practice, Nat. Rev. Clin. Oncol. 18 (1) (2021) 56–62.
[12] Y. Yao, F. Yang, A. Chen, Q. Hua, W. Gao, Costimulatory molecule-related lncRNA model as a potential prognostic biomarker in non-small cell lung cancer, Cancer Med. 12 (5) (2023) 6419–6436.
[13] K. Mi, F. Chen, Z. Qian, J. Chen, D. Lv, C. Zhang, Y. Xu, H. Wang, Y. Zhang, Y. Jiang, D. Shang, Characterizing heterogeneity of non-small cell lung tumour microenvironment to identify signature prognostic genes, J. Cell Mol. Med. 24 (24) (2020) 14608–14618.
[14] M.D. Wilkerson, D.N. Hayes, ConsensusClusterPlus: a class discovery tool with confidence assessments and item tracking, Bioinformatics 26 (12) (2010) 1572–1573.
[15] M. Zhang, K. Zhu, H. Pu, Z. Wang, H. Zhao, J. Zhang, Y. Wang, An immune-related signature predicts survival in patients with lung adenocarcinoma, Front. Oncol. 9 (2019) 1314.
[16] W. Yang, J. Soares, P. Greninger, E.J. Edelman, H. Lightfoot, S. Forbes, N. Bindal, D. Beare, J.A. Smith, I.R. Thompson, S. Ramaswamy, P.A. Futreal, D.A. Haber, M.R. Stratton, C. Benes, U. McDermott, M.J. Garnett, Genomics of Drug Sensitivity in Cancer (GDSC): a resource for therapeutic biomarker discovery in cancer cells, Nucleic Acids Res. 41 (Database issue) (2013) D955–D961.
[17] B. Chen, M.S. Khodadoust, C.L. Liu, A.M. Newman, A.A. Alizadeh, Profiling tumor infiltrating immune cells with CIBERSORT, Methods Mol. Biol. 1711 (2018) 243–259.
[18] M.I. Love, W. Huber, S. Anders, Moderated estimation of fold change and dispersion for RNA-seq data with DESeq2, Genome Biol. 15 (12) (2014) 550.
[19] G. Yu, L.G. Wang, Y. Han, Q.Y. He, clusterProfiler: an R package for comparing biological themes among gene clusters, OMICS 16 (5) (2012) 284–287.
[20] T. Xu, T. Dai, P. Zeng, Q. Song, K. He, Z. Hu, Y. Li, Z. Li, Identification of RHEX as a novel biomarker related to progression and immunity of non-small cell lung carcinoma, Transl. Cancer Res. 10 (8) (2021) 3811–3828.
[21] S. Tang, C. Qin, H. Hu, T. Liu, Y. He, H. Guo, H. Yan, J. Zhang, S. Tang, H. Zhou, Immune checkpoint inhibitors in non-small cell lung cancer: progress, challenges, and prospects, Cells 11 (3) (2022).
[22] S.L. Topalian, J.M. Taube, D.M. Pardoll, Neoadjuvant checkpoint blockade for cancer immunotherapy, Science 367 (6477) (2020).
[23] P. Liao, H. Wang, Y.L. Tang, Y.J. Tang, X.H. Liang, The common costimulatory and coinhibitory signaling molecules in head and neck squamous cell carcinoma, Front. Immunol. 10 (2019) 2457.
[24] Z. Cai, X. Deng, J. Jia, D. Wang, G. Yuan, Ectodysplasin A/ectodysplasin A receptor system and their roles in multiple diseases, Front. Physiol. 12 (2021) 788411.
[25] S. Li, J. Zhou, L. Zhang, J. Li, J. Yu, K. Ning, Y. Qu, H. He, Y. Chen, P.S. Reinach, C.Y. Liu, Z. Liu, W. Li, Ectodysplasin A regulates epithelial barrier function through sonic hedgehog signalling pathway, J. Cell Mol. Med. 22 (1) (2018) 230–240.
[26] Y. Ma, X. Zhang, J. Yang, Y. Jin, Y. Xu, J. Qiu, Comprehensive molecular analyses of a TNF family-based gene signature as a potentially novel prognostic biomarker for cervical cancer, Front. Oncol. 12 (2022) 854615.

[27] B. Wang, Y. Liang, X. Chai, S. Chen, Z. Ye, R. Li, X. Li, G. Kong, Y. Li, X. Zhang, Z. Che, Y. You, S. Ye, L. Li, B. Lin, J. Huang, M. Huang, X. Zhang, X. Qiu, J. Zeng, Ectodysplasin A receptor (EDAR) promotes colorectal cancer cell proliferation via regulation of the Wnt/beta-catenin signaling pathway, Exp. Cell Res. 395 (1) (2020) 112170.
[28] D.J. Headon, S.A. Emmal, B.M. Ferguson, A.S. Tucker, M.J. Justice, P.T. Sharpe, J. Zonana, P.A. Overbeek, Gene defect in ectodermal dysplasia implicates a death domain adapter in development, Nature 414 (6866) (2001) 913–916.
[29] S.H. Seo, S.G. Kim, J.H. Shin, D.W. Ham, E.H. Shin, Toxoplasma GRA16 inhibits NF-kappaB activation through PP2A-B55 upregulation in non-small-cell lung carcinoma cells, Int. J. Mol. Sci. 21 (18) (2020).
[30] F. Amatore, L. Gorvel, D. Olive, Inducible Co-Stimulator (ICOS) as a potential therapeutic target for anti-cancer therapy, Expert Opin. Ther. Targets 22 (4) (2018) 343–351.
[31] J. Monkman, T. Taheri, M. Ebrahimi Warkiani, C. O'Leary, R. Ladwa, D. Richard, K. O'Byrne, A. Kulasinghe, High-plex and high-throughput digital spatial profiling of non-small-cell lung cancer (NSCLC), Cancers 12 (12) (2020).
[32] J.M. Pitt, M. Vetizou, R. Daillere, M.P. Roberti, T. Yamazaki, B. Routy, P. Lepage, I.G. Boneca, M. Chamaillard, G. Kroemer, L. Zitvogel, Resistance mechanisms to immune-checkpoint blockade in cancer: tumor-intrinsic and -extrinsic factors, Immunity 44 (6) (2016) 1255–1269.
[33] V. Ludovini, F. Bianconi, A. Siggillino, J. Vannucci, S. Baglivo, V. Berti, F.R. Tofanetti, M.S. Reda, G. Bellezza, M. Mandarano, M.L. Belladonna, G. Metro, R. Chiari, A. Sidoni, F. Puma, V. Minotti, F. Roila, High PD-L1/Ido-2 and PD-L2/Ido-1 Co-expression levels are associated with worse overall survival in resected non-small cell lung cancer patients, Genes 12 (2) (2021).
[34] L. Yuan, J. Ye, D. Fan, The B7-H4 gene induces immune escape partly via upregulating the PD-1/Stat3 pathway in non-small cell lung cancer, Hum. Immunol. 81 (5) (2020) 254–261.
[35] S.Q. Sun, C.G. Jiang, Y. Lin, Y.L. Jin, P.L. Huang, Enhanced T cell immunity by B7-H4 downregulation in nonsmall-cell lung cancer cell lines, J. Int. Med. Res. 40 (2) (2012) 497–506.
[36] K.A. Schalper, D. Carvajal-Hausdorf, J. McLaughlin, M. Altan, V. Velcheti, P. Gaule, M.F. Sanmamed, L. Chen, R.S. Herbst, D.L. Rimm, Differential expression and significance of PD-L1, Ido-1, and B7-H4 in human lung cancer, Clin. Cancer Res. 23 (2) (2017) 370–378.
[37] Q. Yang, H. Zhang, T. Wei, A. Lin, Y. Sun, P. Luo, J. Zhang, Single-cell RNA sequencing reveals the heterogeneity of tumor-associated macrophage in non-small cell lung cancer and differences between sexes, Front. Immunol. 12 (2021) 756722.
[38] A.J. Patel, A. Richter, M.T. Drayson, G.W. Middleton, The role of B lymphocytes in the immuno-biology of non-small-cell lung cancer, Cancer Immunol. Immunother. 69 (3) (2020) 325–342.
[39] G.H. Ran, Y.Q. Lin, L. Tian, T. Zhang, D.M. Yan, J.H. Yu, Y.C. Deng, Natural killer cell homing and trafficking in tissues and tumors: from biology to application, Signal Transduct Target Ther 7 (1) (2022) 205.
[40] Q. Gu, J. Li, Z. Chen, J. Zhang, H. Shen, X. Miao, Y. Zhou, X. Xu, S. He, Expression and prognostic significance of PD-L2 in diffuse large B-cell lymphoma, Front. Oncol. 11 (2021) 664032.
[41] K.L. Good-Jacobson, C.G. Szumilas, L. Chen, A.H. Sharpe, M.M. Tomayko, M.J. Shlomchik, PD-1 regulates germinal center B cell survival and the formation and affinity of long-lived plasma cells, Nat. Immunol. 11 (6) (2010) 535–542.
[42] T. Calzascia, M. Pellegrini, H. Hall, L. Sabbagh, N. Ono, A.R. Elford, T.W. Mak, P.S. Ohashi, TNF-alpha is critical for antitumor but not antiviral T cell immunity in mice, J. Clin. Invest. 117 (12) (2007) 3833–3845.
[43] K. Wadowska, P. Blasiak, A. Rzechonek, I. Bil-Lula, M. Sliwinska-Mosson, New insights on old biomarkers involved in tumor microenvironment changes and their diagnostic relevance in non-small cell lung carcinoma, Biomolecules 11 (8) (2021).
[44] P. Misra, S. Singh, Role of cytokines in combinatorial immunotherapeutics of non-small cell lung cancer through systems perspective, Cancer Med. 8 (5) (2019) 1976–1995.
[45] K.Y. Hsieh, J.Y. Tsai, Y.H. Lin, F.R. Chang, H.C. Wang, C.C. Wu, Golden berry 4beta-hydroxywithanolide E prevents tumor necrosis factor alpha-induced procoagulant activity with enhanced cytotoxicity against human lung cancer cells, Sci. Rep. 11 (1) (2021) 4610.
[46] Y. Liu, Y. Gao, T. Lin, Expression of interleukin-1 (IL-1), IL-6, and tumor necrosis factor-alpha (TNF-alpha) in non-small cell lung cancer and its relationship with the occurrence and prognosis of cancer pain, Ann. Palliat. Med. 10 (12) (2021) 12759–12766.
[47] Y. Mei, X. Wang, J. Zhang, D. Liu, J. He, C. Huang, J. Liao, Y. Wang, Y. Feng, H. Li, X. Liu, L. Chen, W. Yi, X. Chen, H.M. Bai, X. Wang, Y. Li, L. Wang, Z. Liang, X. Ren, L. Qiu, Y. Hui, Q. Zhang, Q. Leng, J. Chen, G. Jia, Siglec-9 acts as an immune-checkpoint molecule on macrophages in glioblastoma, restricting T-cell priming and immunotherapy response, Nat Cancer 4 (9) (2023) 1273–1291.
[48] C. Claus, C. Ferrara-Koller, C. Klein, The emerging landscape of novel 4-1BB (CD137) agonistic drugs for cancer immunotherapy, mAbs 15 (1) (2023) 2167189.